



Co-variability Between the Broad Absorption Lines and Narrow Absorption Lines

Bo-Lin Qin (覃柏霖)¹, Jing Li (黎静)^{1,2} , and Wei-Jian Lu (陆伟坚)³

¹Guangdong Country Garden School, Foshan 528312, China

²Laboratory for Relativistic Astrophysics, Physical Science and Technology College, Guangxi University, Nanning 530004, China; ginny_lee@qq.com

³School of Information Engineering, Baise University, Baise 533000, China

Received 2024 June 3; revised 2024 August 1; accepted 2024 August 9; published 2024 September 16

Abstract

We investigate the relationship between the variability of broad absorption lines (BALs) or narrow absorption lines (NALs) and that of continuum using a data set of two-epoch SDSS spectra containing 134 C IV NAL-BAL pairs. Our analysis reveals an anti-correlation between the fractional equivalent width (EW) variations in NALs (or BALs) and the fractional flux variations of the continuum, with Spearman rank correlation coefficients of $r = -0.47$ ($p = 1\text{E-}08$) and $r = -0.58$ ($p = 1\text{E-}13$), respectively. In addition, we find a positive correlation between the fractional EW variations in NALs and BALs ($r = 0.72$, $p = 1\text{E-}22$), and derive a regression equation $\Delta\text{EW}_{\text{NAL}}/\langle\text{EW}_{\text{NAL}}\rangle = 0.803\Delta\text{EW}_{\text{BAL}}/\langle\text{EW}_{\text{BAL}}\rangle + 0.008$, with an intrinsic scatter of 0.14. These results suggest that the variability in the ionizing continuum may play a significant role in the observed changes in C IV NALs and BALs, supporting the idea of photoionization-driven variability. The co-variability between C IV NALs and BALs may imply that they originate from outflows with similar physical conditions.

Key words: (galaxies:) quasars: absorption lines – (galaxies:) quasars: general – galaxies: active

1. Introduction

Absorption lines are instrumental in the spectral observation of quasars, providing insight into the physical and chemical composition of media that is either non-luminous or not directly observable due to technological limitations (e.g., Weymann et al. 1998). Based on their physical connection to the quasars, absorption lines are divided into two categories: intervening absorption lines and intrinsic absorption lines. Intervening absorption lines arise from absorbers that are not physically associated with quasars, such as the interstellar medium and insertion galaxies. Intrinsic absorption lines arise from absorbers that are physically associated with quasars, such as gases in the vicinity of outflows or accretion disks (e.g., Barlow et al. 1997; Savage et al. 1998; Chen et al. 2018). The absorption lines are further classified by their line widths: narrow absorption lines (NALs), which have widths of a few hundred km s^{-1} , broad absorption lines (BALs), with widths exceeding 2000 km s^{-1} and depths greater than 10% below the continuum (e.g., Weymann et al. 1991), and mini-BALs, which exhibit line widths between those of NALs and BALs (e.g., Hamann & Sabra 2004; Chen et al. 2021). Intrinsic absorption lines, including BALs, mini-BALs, and NALs, present diverse characteristics, with underlying mechanisms of considerable complexity. Previous studies indicate that the predominant physical mechanisms are likely linked to the diverse inclination angles of the quasar line of sight relative to the accretion disk axis, as well as the distinct evolutionary stages of

the quasar outflow or host galaxy (e.g., Murray et al. 1995; Hamann et al. 2009, 2012; Rodríguez Hidalgo et al. 2013; Chen et al. 2022; Peng et al. 2024).

Absorption lines in quasars exhibit significant variability, a phenomenon observed in both BALs and NALs. Studies have found that the profiles and intensities of BALs can undergo substantial changes on timescales ranging from days to years (e.g., Capellupo et al. 2011, 2012, 2013; Filiz et al. 2012, 2013; Grier et al. 2015; He et al. 2015; Wang et al. 2015), while the strength of intrinsic NALs has also been observed to fluctuate notably over periods of months to years (e.g., Wise et al. 2004; Hamann et al. 2011; Chen & Qin 2013; Hacker et al. 2013; Wang et al. 2015; He et al. 2015; Hemler et al. 2019). BALs are typically associated with high-velocity outflows, which are physically connected to the central regions of quasars, such as the accretion disk and the dusty torus (e.g., He et al. 2022; Naddaf et al. 2023). In contrast, NALs may be located further away, such as in the disk or halo of the galaxy, and their variations may require longer timescales to respond to the changes in the central region (e.g., Barlow et al. 1997). Investigating the correlation between changes in BALs and NALs can enhance our understanding of the physical relationship of both types of absorption lines. Although numerous studies on the variability of BALs and NALs over the years, investigations into the correlation between the variability of these two types of absorption lines remain scarce.

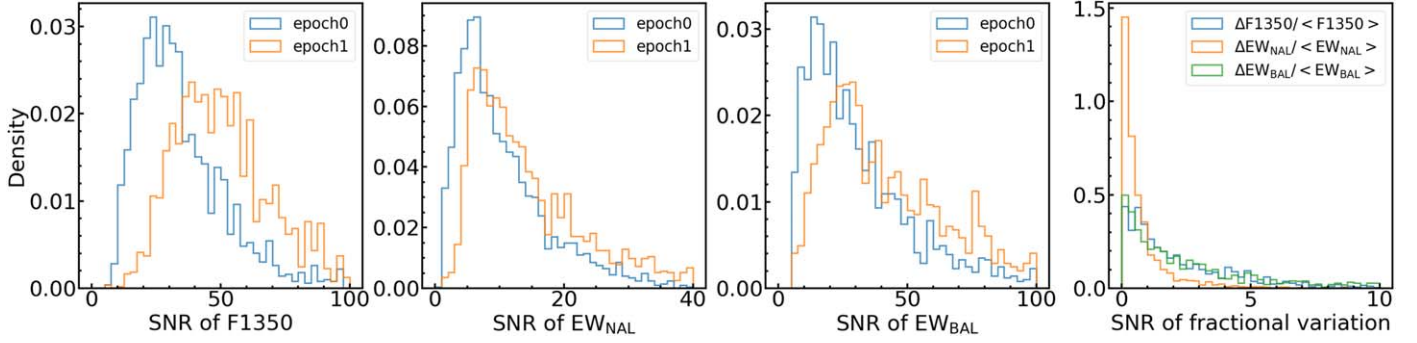


Figure 1. The signal-to-noise ratio distribution of our data.

It is acknowledged that two primary mechanisms underlie the changes observed in absorption lines: variations in the ionization state of the absorbing gas (e.g., Barlow 1994; Hamann et al. 2011; Filiz et al. 2014; He et al. 2015; Wang et al. 2015; Lu et al. 2017; Chen et al. 2018b; Vivek 2019; Zhao et al. 2021; Lin et al. 2024) and alterations in the covering factor of the absorbers relative to the central continuum source (e.g., Narayanan et al. 2004; Lundgren et al. 2007; Hamann et al. 2008; Krongold et al. 2010; Hall et al. 2011; Filiz et al. 2012; Capellupo et al. 2013; Vivek et al. 2016; Capellupo et al. 2017). Changes in the ionization state of absorbers can directly affect its absorption properties. Quasar variability significantly affects the ambient environment, modifying the absorbers' physical properties, including ionization state, density, and temperature. The intrinsic absorbers' close association with the quasar center means that variations in quasar activity directly alter the ionization structure of the absorbers, leading to changes in their ionization states and densities, and thus in the absorption lines. In addition, alterations in the covering factor of the absorbing gas relative to the central continuum source can also occur, impacting the strength and profile of the absorption lines. The bulk motion of the absorbers, the rotational motion of outflows, or changes in the internal velocity structure of the outflows can induce variations in the covering factor, which in turn affect the characteristics of the absorption lines. Determining the predominant mechanism between these two currently is difficult, as some sources may be primarily influenced by the first mechanism, while others are more likely influenced by the second. The possibility of both mechanisms contributing to the observed variations cannot be ruled out (e.g., Lundgren et al. 2007; Capellupo et al. 2011; Vivek et al. 2014).

In this paper, We first study the correlation between the variability of the C IV BALs and the continuum, as well as between the variability of the C IV NALs and the continuum. Then we analyze the correlation between the variability of the C IV BALs and NALs. In addition, we explore the physical processes that lead to changes in quasar absorption lines and

the mechanisms that classify them into BAL, mini-BAL, and NALs. Section 2 provides a description of the sample, Section 3 entails an analysis of the data, and Section 4 presents the results and discussion. In Section 5 we draw conclusions.

2. Sample

The sample for this study is derived from the previous works of He et al. (2017) and Chen et al. (2018b). He et al. (2017) provided a catalog containing 9918 pairs of spectra with C IV BALs, which were obtained from a sample of 2005 BAL quasars selected from the Sloan Digital Sky Survey (SDSS). Chen et al. (2018b) presented a catalog consisting of 21,239 C IV NAL systems, detected from the spectra of 13,769 quasars observed by SDSS. In this study, we first cross-matched these two catalogs to get the common quasars. Then, we selected the quasars with two-epoch observations and obtained the corresponding spectra. Subsequently, we selected the spectra that contain both C IV NALs and C IV BALs, to form NAL-BAL pairs. We finally obtained 2119 NAL-BAL pairs from 1059 quasars with two-epoch observations.

To obtain reliable analytical results, we require the data to have a high signal-to-noise ratio (SNR). As shown in Figure 1, the peak SNRs for F1350 across two observations approximate 25 and 40, respectively, as depicted in Figure 1. For the EW of C IV NALs, the peak SNRs for both observations are approximately 6, as shown in Figure 2. For the EW of C IV BALs, the peak SNRs for the previous and later observations are approximately 13 and 20, respectively, as shown in Figure 3. In subsequent analyses, we only adopted the data with an SNR greater than the distribution peak. Furthermore, we performed a data filtering process to eliminate measurements with fractional variations smaller than their uncertainties, as these data were considered unreliable. After the filtering process, we retained a total sample of 134 NAL-BAL pairs for further analysis.

At the same time, we identified two types of NAL-BAL pairs through visual inspection, as illustrated in Figure 2. One type consists of an NAL located outside the BAL trough, while the

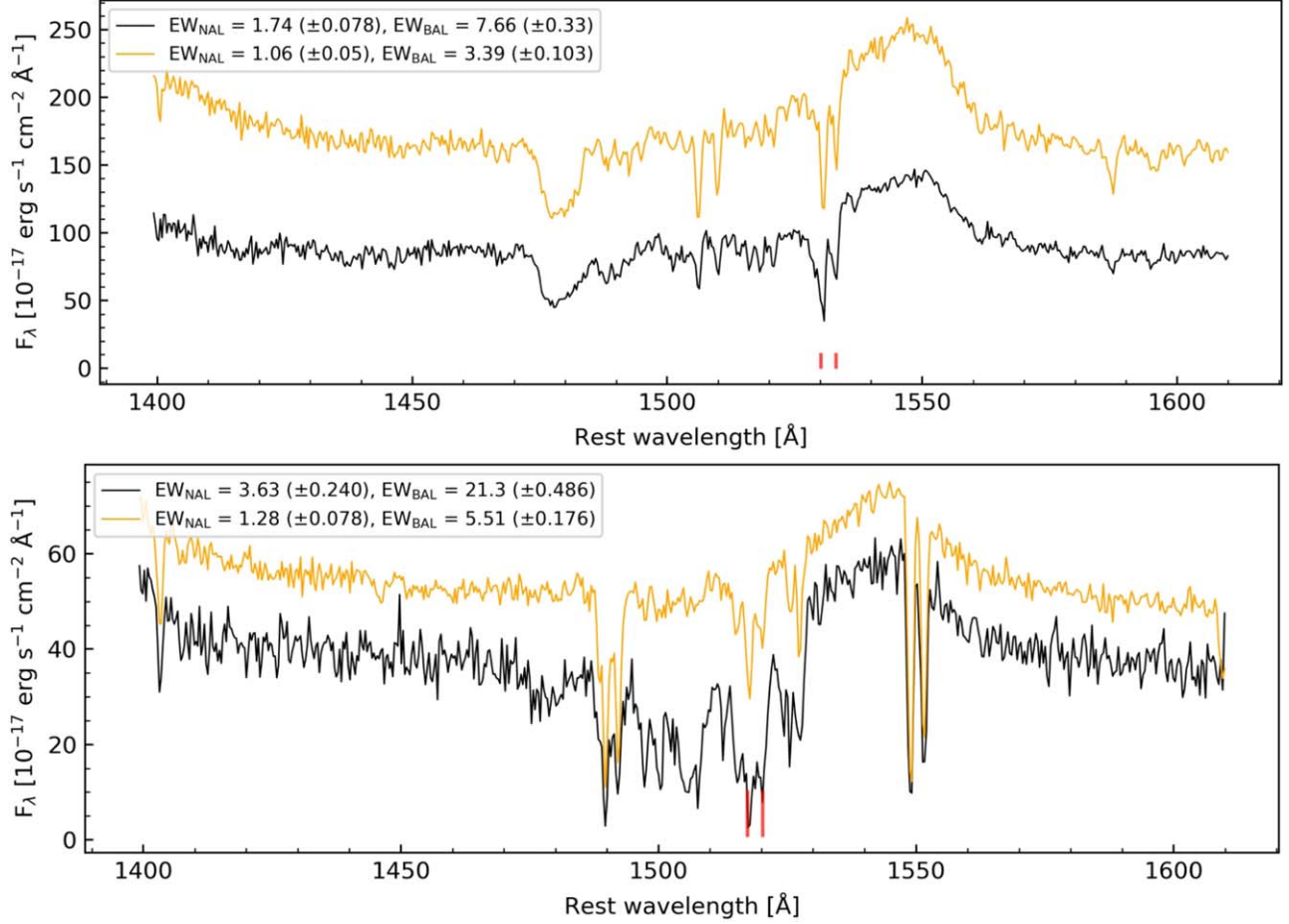


Figure 2. Examples of two types of NAL-BAL pairs. The top panel presents a Type I example (SDSS J102009.99+104002.7), the black and orange lines indicate the previous and later observations (MJD = 52999 and MJD = 55957), respectively. The bottom panel illustrates a Type II example (SDSS J134544.55+002810.7), with the black and orange lines representing the previous and later observations (MJD = 51943 and MJD = 55630), respectively. In both panels, the red vertical lines mark the position of the C IV NALs. The rest EWs of the C IV NALs are shown in the upper left corner of each panel.

other type includes a NAL positioned within the BAL trough. We categorized these two types of NAL-BAL pairs as Type I and Type II, respectively.

3. Data Analysis

3.1. The Variability of NALs and BALs

He et al. (2017) has shown that the equivalent width (EW) of C IV NALs are influenced by the ionization parameter U , with a pattern of initially increasing, reaching a peak, and subsequently decreasing. Following Lu et al. (2018), we utilized the fractional variations of EW to estimate the variability of NALs and BALs. The fractional variation of equivalent width is defined as:

$$\frac{\Delta \text{EW}}{\langle \text{EW} \rangle} = \frac{\text{EW}_2 - \text{EW}_1}{(\text{EW}_2 + \text{EW}_1) \times 0.5}, \quad (1)$$

where EW_1 and EW_2 represent the EW of previous and later observations, respectively. Correspondingly, the uncertainty of $\frac{\Delta \text{EW}}{\langle \text{EW} \rangle}$ is defined as:

$$\sigma_{\frac{\Delta \text{EW}}{\langle \text{EW} \rangle}} = \frac{4\sqrt{\text{EW}_2^2 \sigma_{\text{EW}_1}^2 + \text{EW}_1^2 \sigma_{\text{EW}_2}^2}}{(\text{EW}_2 + \text{EW}_1)^2}, \quad (2)$$

where σ_{EW_1} and σ_{EW_2} represent the uncertainties of EW in the previous and later observations, respectively. The EW and σ_{EW} measurements of C IV BALs and NALs were derived from He et al. (2017) and Chen et al. (2018b), respectively.

3.2. The Variability of Power-law Continuum

Similarly, we computed the the fractional variations of continuum flux at 1350 in rest-frame (F1350) to estimate the variability of power-law continuum. The the fractional

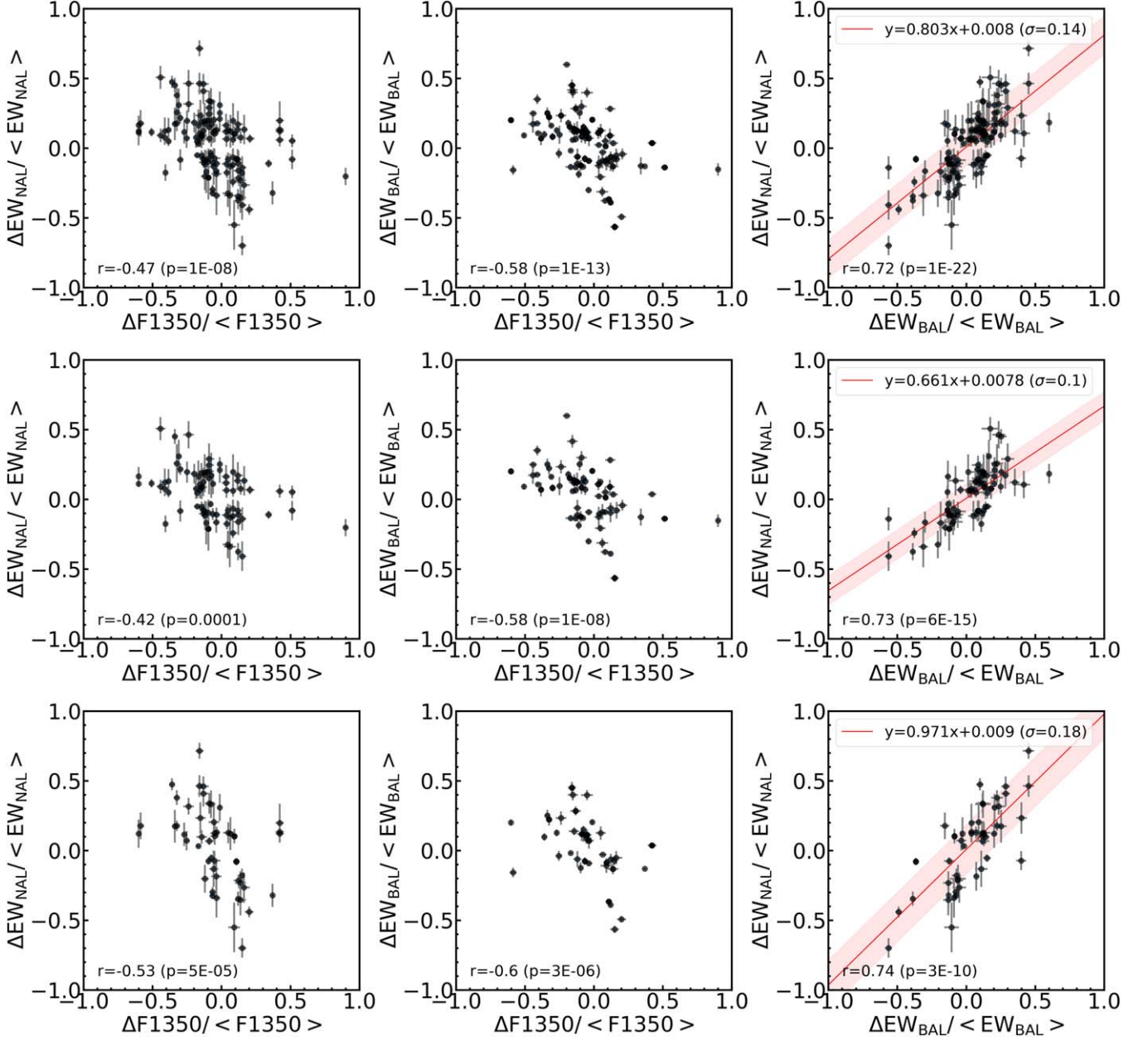


Figure 3. Correlation between the fractional variations of F1350, EW_{BAL} and EW_{NAL}. The subfigures in the first, second and third rows represent the results of the total sample, Type I sample and Type II sample. The values in the lower left corner denote the Spearman correlation coefficients and their corresponding p -values. The red line indicates the results of the Bayesian linear regression analysis (Kelly 2007).

variations of continuum is defined as:

$$\frac{\Delta F_{\text{cont}}}{\langle F_{\text{cont}} \rangle} = \frac{F_{\text{cont}2} - F_{\text{cont}1}}{(F_{\text{cont}2} + F_{\text{cont}1}) \times 0.5}, \quad (3)$$

where $F_{\text{cont}1}$ and $F_{\text{cont}2}$ represent the F1350 of previous and later observations, respectively. Correspondingly, the

uncertainty of $\frac{\Delta F_{\text{cont}}}{\langle F_{\text{cont}} \rangle}$ is defined as:.

$$\sigma_{\frac{\Delta F_{\text{cont}}}{\langle F_{\text{cont}} \rangle}} = \frac{4\sqrt{F_{\text{cont}2}^2 \sigma_{F_{\text{cont}1}}^2 + F_{\text{cont}1}^2 \sigma_{F_{\text{cont}2}}^2}}{(F_{\text{cont}2} + F_{\text{cont}1})^2}, \quad (4)$$

where $\sigma_{F_{\text{cont}1}}$ and $\sigma_{F_{\text{cont}2}}$ represent the uncertainties of F1350 in the previous and later observations, respectively. We also adopted the F_{cont} and $\sigma_{F_{\text{cont}}}$ measurements from He et al. (2017) and Chen et al. (2018b).

Table 1
The Spearman Rank Correlation Analysis Results of Different Samples

| | $r(p)$ The Total Sample | $r(p)$ Type I Sample | $r(p)$ Type II Sample |
|--|----------------------------|-------------------------|--------------------------|
| $\Delta EW_{\text{NAL}}/\langle EW_{\text{NAL}} \rangle$ versus $\Delta F1350/\langle F1350 \rangle$ | −0.47 (1E-08) | −0.42 (1E-04) | −0.53 (5E-05) |
| $\Delta EW_{\text{BAL}}/\langle EW_{\text{BAL}} \rangle$ versus $\Delta F1350/\langle F1350 \rangle$ | −0.58 (1E-13) | −0.58 (1E-08) | −0.60 (3E-06) |
| $\Delta EW_{\text{BAL}}/\langle EW_{\text{BAL}} \rangle$ versus $\Delta EW_{\text{NAL}}/\langle EW_{\text{NAL}} \rangle$ | 0.72 (1E-22) | 0.73 (6E-15) | 0.74 (3E-10) |

4. Results and Discussion

Based on the sample obtained in Section 2, we plotted the fractional EW variation of CIV NALs (or BALs) versus the fractional variation of F1350, as well as the fractional EW variation between CIV NALs and CIV BALs, as shown in Figure 3. The Spearman rank correlation analyses for different samples are presented in Table 1.

First, we find that the fractional EW variations of both the CIV NALs and CIV BALs are inversely correlated with the fractional flux variations of the continuum across all samples, as demonstrated in the left and middle column Subfigures of Figure 3. This inverse correlation has been previously reported, several studies discovered an inverse correlation between the fractional EW variations of NALs and the fractional flux variations of the continuum (e.g., Lu et al. 2017; Chen et al. 2018b). Meanwhile, some studies reported similar relationships for BALs (e.g., Lu & Lin 2018b; Lu et al. 2018; Huang et al. 2019; Mishra et al. 2021; Lin et al. 2024). In our study, we consider that the variations in both BALs and NALs are primarily driven by changes in the ionizing continuum, which alters the ionization state or column density of the relevant metal ions (e.g., Crenshaw et al. 2003; Wise et al. 2004; Hamann et al. 2011; Misawa et al. 2014; Wang et al. 2015; He et al. 2017; Vivek 2019). Photoionization simulations show the EWs of the absorption lines first rise, reach a peak, and then decline with increasing ionization parameter (U), dividing into low and high ionization states. In the low ionization states, the absorption lines positively respond to central source variations, while in the high ionization states, they show a negative response. It suggests that the majority of BALs and NALs investigated herein might reside in a relatively highly ionized state, originating from absorption clouds dominated by high-ionization gas. Relevant researches show that the detectability of NALs or BALs variations hinges on the gas' recombination timescale being shorter than the detection interval (e.g., Krolik & Kriss 1995; He et al. 2019). The variations in BALs and NALs are negatively correlated with changes in central radiation, possibly due to the asymmetric recombination timescale effects. According to He & Wang (2023), absorbers with high ionization states exhibit shorter response timescales compared to those with low ionization states, leading to the detection of more negative responses. The NAL and BAL that can be detected may be only the parts with extremely high

ionization states and therefore shorter recombination timescales. Our results are consistent with previous studies.

Second, we present the correlation between the EW variations of BALs and NALs, as illustrated in the right column of Figure 3. Although previous works have explored the relationship between variations in BALs and changes in the continuum, as well as the relationship between NALs' variations and continuum's changes, there remains a gap in research concerning the relationship between variations in BALs and that of NALs. In our results (the right column of Figure 3), the EW variations of BALs and NALs exhibit a significant positive correlation. This correlation suggests that BALs and NALs may originate from the outflow with similar physical conditions. According to the inclination hypothesis, different types of absorption lines represent the same outflow observed at different angles, with BALs forming in the main body of the outflow close to the accretion disk plane, while NALs and mini-BALs form along sightlines that graze the edges of the outflows at higher latitudes above the disk plane (e.g., Murray et al. 1995; Proga & Kallman 2004; Ganguly et al. 2001; Chartas et al. 2009; Hamann et al. 2012). If the inclination hypothesis holds, the simultaneous presence of BALs and NALs within the same spectrum in our sample may suggest that there might not be a distinct boundary between sightline angles that produce solely BALs or solely NALs. Instead, there could be a region where both BALs and NALs are observed, as reported by Itoh et al. (2020). According to the evolution hypothesis, NALs and mini-BALs might represent either the initial or late phases of a powerful outflow, implying that BALs and NALs may denote different evolutionary stages of the same outflow (e.g., Hamann et al. 2008; Gibson et al. 2010; Rodríguez Hidalgo et al. 2013). Given the previously discussed, the observed variations in both BALs and NALs are primarily influenced by photoionization, and CIV BALs and NALs are in similar ionized states, it is unlikely that these two types of absorption lines arise from absorbers at different stages of evolution. Consequently, our findings are more conducive to the inclination hypothesis rather than the evolutionary hypothesis.

Third, our results show that the EWs of Type I pairs and Type II pairs show consistency in their variations with the changes in the continuum flux. It indicates that there may be some physical relationship between them, such as originating

from high-ionization outflow gases close to the central engine. The difference is that BALs typically originate from the large-scale clumpy structure or a large number of small-scale clumpy structure of the outflow, while NALs primarily stem from the small-scale clumpy structure of the outflow (e.g., Hamann et al. 2011; Itoh et al. 2020). In addition, Lu & Lin (2018a) and Lu & Lin (2019) identified NALs within broad absorption troughs, suggesting that there may be two types of BALs: one that cannot be decomposed into NALs and the other that is a blend of NALs, which can be decomposed into NALs with similar intrinsic properties. Our findings are in agreement with this perspective.

5. Conclusion

We have studied the correlation between the variability of NALs (or BALs) and the continuum's variability using a sample of two-epoch SDSS spectra containing 134 NAL-BAL pairs. The fractional EW variations in NALs and BALs correlate with the fractional variations in the continuum flux, with Spearman rank correlation coefficient $r = -0.47$ ($p = 1\text{E-}08$) and $r = -0.58$ ($p = 1\text{E-}13$), respectively. Additionally, there is a correlation between the fractional EW variations in NALs and BALs ($r = 0.72$, $p = 1\text{E-}22$). A regression equation $\Delta\text{EW}_{\text{NAL}}/\langle\text{EW}_{\text{NAL}}\rangle = 0.803\Delta\text{EW}_{\text{BAL}}/\langle\text{EW}_{\text{BAL}}\rangle + 0.008$ with an intrinsic scatter of 0.14 has been obtained. Based on these results, we draw the following conclusions.

(1) The fractional EW variations of both CIV NALs and BALs in our study are inversely correlated with the fractional flux variations of the continuum, suggesting that the variations in both NALs and BALs are primarily driven by changes in the ionizing continuum, which alter the ionization state or column density of the relevant metal ions.

(2) Utilizing data from quasars exhibiting both NALs and BALs, our results indicate a significant positive correlation between the fractional EW variations of BALs and NALs, suggesting that BALs and NALs may originate from outflows with similar physical conditions, which favors the inclination hypothesis rather than the evolution hypothesis.

(3) Our results show consistency in the fractional variations of the EWs of Type I pairs and Type II pairs with the changes in the continuum flux, which may indicate some physical relationship between them.

Acknowledgments

We thank He et al. and Chen et al. for making their data public. We also thank Ying-Ru Lin and Min Yao (Baise University, Guangxi Baise, China) for useful discussions. This research was supported by the Guangxi Natural Science Foundation (No. 2021GXNSFBA220044), the National Natural Science Foundation of China (No. 11903002), and the Research Project of Baise University (No. 2019KN04).

Funding for the Sloan Digital Sky Survey IV was provided by the Alfred P. Sloan Foundation, the U.S. Department of Energy Office of Science, and the Participating Institutions. SDSS-IV acknowledges support and resources from the Center for High-Performance Computing at the University of Utah. The SDSS website is <http://www.sdss.org/>.

SDSS-IV is managed by the Astrophysical Research Consortium for the Participating Institutions of the SDSS Collaboration including the Brazilian Participation Group, the Carnegie Institution for Science, Carnegie Mellon University, the Chilean Participation Group, the French Participation Group, Harvard-Smithsonian Center for Astrophysics, Instituto de Astrofísica de Canarias, The Johns Hopkins University, Kavli Institute for the Physics and Mathematics of the Universe (IPMU)/University of Tokyo, Lawrence Berkeley National Laboratory, Leibniz Institut für Astrophysik Potsdam (AIP), Max-Planck-Institut für Astronomie (MPIA Heidelberg), Max-Planck-Institut für Astrophysik (MPA Garching), Max-Planck-Institut für Extraterrestrische Physik (MPE), National Astronomical Observatories of China, New Mexico State University, New York University, University of Notre Dame, Observatório Nacional/MCTI, The Ohio State University, Pennsylvania State University, Shanghai Astronomical Observatory, United Kingdom Participation Group, Universidad Nacional Autónoma de México, University of Arizona, University of Colorado Boulder, University of Oxford, University of Portsmouth, University of Utah, University of Virginia, University of Washington, University of Wisconsin, Vanderbilt University, and Yale University.

Author Contributions: W.-J.L. conceived the initial idea. B.-L.Q. and J.L. co-developed the idea and led the data analysis. J.L. and B.-L.Q. led the interpretation and manuscript writing.

ORCID iDs

Jing Li (黎静)  <https://orcid.org/0009-0001-4875-1079>

Wei-Jian Lu (陆伟坚)  <https://orcid.org/0000-0002-1185-4146>

References

- Barlow, T. A. 1994, *PASP*, **106**, 548
- Barlow, T. A., Hamann, F., & Sargent, W. L. W. 1997, in ASP Conf. Ser. 128, Mass Ejection from Active Galactic Nuclei, ed. N. Arav, I. Shlosman, & R. J. Weymann (San Francisco, CA: ASP), 13
- Capellupo, D. M., Hamann, F., Shields, J. C., Halpern, J. P., & Barlow, T. A. 2013, *MNRAS*, **429**, 1872
- Capellupo, D. M., Hamann, F., Shields, J. C., Rodríguez Hidalgo, P., & Barlow, T. A. 2011, *MNRAS*, **413**, 908
- Capellupo, D. M., Hamann, F., Shields, J. C., Rodríguez Hidalgo, P., & Barlow, T. A. 2012, *MNRAS*, **422**, 3249
- Capellupo, D. M., Hamann, F., Herbst, H., et al. 2017, *MNRAS*, **469**, 323
- Chartas, G., Charlton, J., Eracleous, M., et al. 2009, *NewAR*, **53**, 128
- Chen, C., Hamann, F., Ma, B., & Murphy, M. 2021, *ApJ*, **907**, 84
- Chen, C., Hamann, F., Simon, L., & Barlow, T. 2018, *MNRAS*, **481**, 3865
- Chen, Z.-F., & Qin, Y.-P. 2013, *ApJ*, **777**, 56

- Chen, Z.-F., Yao, M., Pang, T.-T., et al. 2018b, [ApJS](#), **239**, 23
- Chen, Z., He, Z., Ho, L. C., et al. 2022, [NatAs](#), **6**, 339
- Crenshaw, D. M., Kraemer, S. B., & George, I. M. 2003, [ARA&A](#), **41**, 117
- Filiz, A. N., Brandt, W. N., Hall, P. B., et al. 2012, [ApJ](#), **757**, 114
- Filiz, A. N., Brandt, W. N., Hall, P. B., et al. 2013, [ApJ](#), **777**, 168
- Filiz, A. N., Brandt, W. N., Hall, P. B., et al. 2014, [ApJ](#), **791**, 88
- Ganguly, R., Bond, N. A., Charlton, J. C., et al. 2001, [ApJ](#), **549**, 133
- Gibson, R. R., Brandt, W. N., Gallagher, S. C., Hewett, P. C., & Schneider, D. P. 2010, [ApJ](#), **713**, 220
- Grier, C. J., Hall, P. B., Brandt, W. N., et al. 2015, [ApJ](#), **806**, 111
- Hacker, T. L., Brunner, R. J., Lundgren, B. F., & York, D. G. 2013, [MNRAS](#), **434**, 163
- Hall, P. B., Anosov, K., White, R. L., et al. 2011, [MNRAS](#), **411**, 2653
- Hamann, F., Kanekar, N., Prochaska, J. X., et al. 2011, [MNRAS](#), **410**, 1957
- Hamann, F., Kaplan, K. F., Rodríguez Hidalgo, P., Prochaska, J. X., & Herbert-Fort, S. 2008, [MNRAS](#), **391**, L39
- Hamann, F., & Sabra, B. 2004, in ASP Conf. Ser. 311, AGN Physics with the Sloan Digital Sky Survey, ed. G. T. Richards & P. B. Hall (San Francisco, CA: ASP), 203
- Hamann, F., Simon, L., Rodríguez Hidalgo, P., & Capellupo, D. 2012, in ASP Conf. Ser. 460, AGN Winds in Charleston, ed. G. Chartas, F. Hamann, & K. M. Leighly (San Francisco, CA: ASP), 47
- Hamann, F. W., Kaplan, K. F., Rodríguez Hidalgo, P., Prochaska, J. X., & Herbert-Fort, S. 2009, AAS Meeting , 213, 446.12
- He, Z.-C., Bian, W.-H., Ge, X., & Jiang, X.-L. 2015, [MNRAS](#), **454**, 3962
- He, Z., & Wang, T. 2023, [arXiv:2311.16463](#)
- He, Z., Wang, T., Zhou, H., et al. 2017, [ApJS](#), **229**, 22
- He, Z., Wang, T., Liu, G., et al. 2019, [NatAs](#), **3**, 265
- He, Z., Liu, G., Wang, T., et al. 2022, [SciA](#), **8**, eabk3291
- Hemler, Z. S., Grier, C. J., Brandt, W. N., et al. 2019, [ApJ](#), **872**, 21
- Huang, H.-Y., Pan, C.-J., Lu, W.-J., et al. 2019tpdel, [MNRAS](#), **487**, 2818
- Itoh, D., Misawa, T., Horiuchi, T., & Aoki, K. 2020, [MNRAS](#), **499**, 3094
- Kelly, B. C. 2007, [ApJ](#), **665**, 1489
- Krolik, J. H., & Kriss, G. A. 1995, [ApJ](#), **447**, 512
- Krongold, Y., Binette, L., & Hernández-Ibarra, F. 2010, [ApJL](#), **724**, L203
- Lin, Y.-R., Pan, C.-J., & Lu, W.-J. 2024, [RAA](#), **24**, 025016
- Lu, W.-J., & Lin, Y.-R. 2018a, [MNRAS](#), **474**, 3397
- Lu, W.-J., & Lin, Y.-R. 2018b, [ApJ](#), **862**, 46
- Lu, W.-J., & Lin, Y.-R. 2019, [ApJ](#), **881**, 105
- Lu, W.-J., Lin, Y.-R., & Qin, Y.-P. 2018, [MNRAS](#), **473**, L106
- Lu, W.-J., Lin, Y.-R., Qin, Y.-P., et al. 2017, [MNRAS](#), **468**, L6
- Lundgren, B. F., Wilhite, B. C., Brunner, R. J., et al. 2007, [ApJ](#), **656**, 73
- Misawa, T., Charlton, J. C., & Eracleous, M. 2014, [ApJ](#), **792**, 77
- Mishra, S., Vivek, M., Chand, H., & Joshi, R. 2021, [MNRAS](#), **504**, 3187
- Murray, N., Chiang, J., Grossman, S. A., & Voit, G. M. 1995, [ApJ](#), **451**, 498
- Naddaf, M. H., Martínez-Aldama, M. L., Marziani, P., et al. 2023, [A&A](#), **675**, A43
- Narayanan, D., Hamann, F., Barlow, T., et al. 2004, [ApJ](#), **601**, 715
- Peng, X.-L., Chen, Z.-F., He, Z.-C., Pang, T.-T., & Wang, Z.-W. 2024, [ApJ](#), **963**, 3
- Proga, D., & Kallman, T. R. 2004, [ApJ](#), **616**, 688
- Rodríguez Hidalgo, P., Eracleous, M., Charlton, J., et al. 2013, [ApJ](#), **775**, 14
- Savage, B. D., Tripp, T. M., & Lu, L. 1998, [AJ](#), **115**, 436
- Vivek, M. 2019, [MNRAS](#), **486**, 2379
- Vivek, M., Srianand, R., & Gupta, N. 2016, [MNRAS](#), **455**, 136
- Vivek, M., Srianand, R., Petitjean, P., et al. 2014, [MNRAS](#), **440**, 799
- Wang, T., Yang, C., Wang, H., & Ferland, G. 2015, [ApJ](#), **814**, 150
- Weymann, R. J., Morris, S. L., Foltz, C. B., & Hewett, P. C. 1991, [ApJ](#), **373**, 23
- Weymann, R. J., Jannuzi, B. T., Lu, L., et al. 1998, [ApJ](#), **506**, 1
- Wise, J. H., Eracleous, M., Charlton, J. C., & Ganguly, R. 2004, [ApJ](#), **613**, 129
- Zhao, Q., He, Z., Liu, G., et al. 2021, [ApJL](#), **906**, L8